Air Entrainment and Scale Effects in Hydraulic Jumps with Small Froude Numbers

Y. Chachereau[1] and H. Chanson[1]
[1]School of Civil Engineering
The University of Queensland
Brisbane QLD 4072
AUSTRALIA
E-mail: h.chanson@uq.edu.au

Abstract: *The transition from supercritical to subcritical flow is characterised by a strong dissipative mechanism, a hydraulic jump. In the present study, the air-water properties were investigated experimentally in hydraulic jumps with relatively small Froude numbers ($2.4 < Fr_1 < 5.1$) and relatively large Reynolds numbers. A comparative analysis demonstrated that, for hydraulic jumps with $Fr_1 = 5.1$, the void fraction data obtained with $Re < 4 \times 10^4$ could not be scaled up to $Re = 1 \times 10^5$. Most air-water flow properties measured with Reynolds numbers up to 1.25×10^5 could not be extrapolated to large-size prototype structures without significant scale effects in terms of bubble count rate, turbulence and bubble chord time distributions. The findings have some major implications of civil, environmental and sanitary engineering designs, because most hydraulic structures, storm water systems and water treatment facilities operate with Reynolds numbers larger than 10^6 to over 10^8.*

Keywords: *Hydraulic jumps, Air entrainment, Dynamic similarity, Physical modelling, Scale effects.*

1. INTRODUCTION

An open channel flow can change from subcritical to supercritical in a relatively smooth manner at gates and weir crests. The flow regime evolves from subcritical to supercritical with the occurrence of critical flow conditions associated with relatively small energy loss (e.g. broad-crested weir) (Henderson 1966). The transition from supercritical to subcritical flow is, on the other hand, characterised by a strong dissipative mechanism. It is called a hydraulic jump (Fig. 1). A hydraulic jump is extremely turbulent. It is characterised by the development of large-scale turbulence, surface waves and spray, energy dissipation and air entrainment. A hydraulic jump is a region of rapidly-varied flow and the large-scale turbulence region is usually called the roller. The flow within a hydraulic jump remains a challenge to scientists and researchers (Rajaratnam 1962, Hager 1992, Chanson 2009).

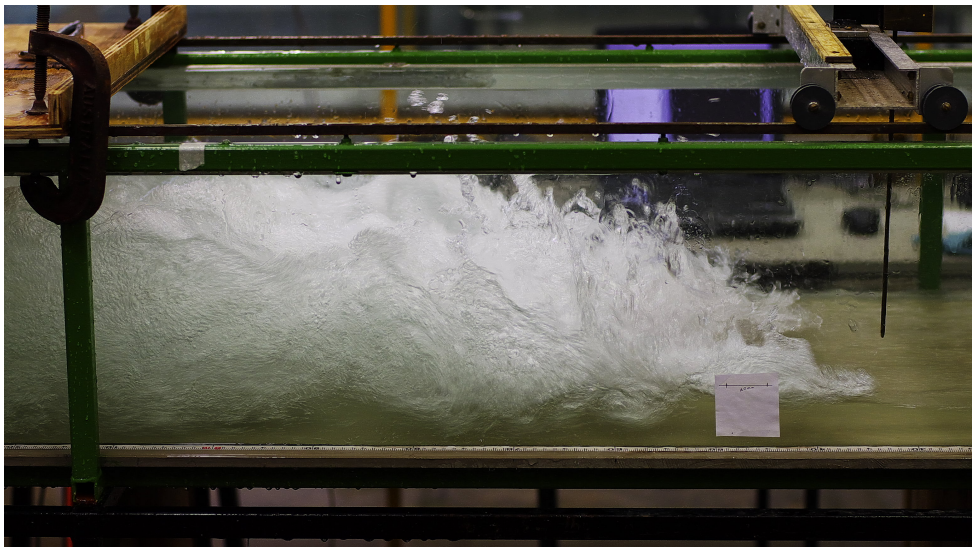

Fig. 1 - Air entrainment in a hydraulic jump: $d_1 = 0.0395$ m, $Fr_1 = 5.1$, $Re = 1.3 \times 10^5$ - Flow from right to left

The present study aims to examine accurately the air-water flow properties in hydraulic jumps with relatively small Froude numbers ($2.4 < Fr_1 < 5.1$) operating at relatively large Reynolds numbers ($6.6\times10^4 < Re < 1.3\times10^5$). For a Froude number $Fr_1 = 5.1$, the present results were compared with earlier data obtained with the same Froude number but smaller Reynolds numbers ($2.5\times10^4 < Re < 6.8\times10^4$). The results are discussed in terms of the Froude similarity.

1.1. Dimensional considerations and physical modelling

The experimental investigations of hydraulic jumps are not simple but some new advances in metrology and signal processing provided the means for successful air-water turbulent flow measurements in hydraulic jumps (e.g. Mossa and Tolve 1998, Chanson and Brattberg 2000, Murzyn et al. 2005). The physical studies are performed with geometrically similar models and the selection of an adequate similitude is critical. The relevant parameters needed for any dimensional analysis include the fluid properties and physical constants, the channel geometry and inflow conditions, and the air-water flow properties including the entrained air bubble characteristics (Chanson and Gualtieri 2008). The biochemical properties of the water solution may be considered and compressibility of high-velocity air–water flow might be relevant. In free-surface flows, the compressibility effects have little impact on air bubble diffusion process and on mixing layer characteristics (Chanson 1997), and these are not considered herein. Further, the density and viscosity of the air-water mixture can be estimated from the water properties and local void fraction.

In a hydraulic jump, the characteristic length scale is the upstream flow depth d_1. A simplified dimensional analysis yields:

$$C, \frac{V}{V_1}, \frac{u'}{V_1}, \frac{d_{ab}}{d_1}, \frac{F\,d_1}{V_1}, ... = f_2\left(\frac{x-x_1}{d_1}, \frac{y}{d_1}, \frac{z}{d_1}, \frac{x_1}{d_1}, \frac{u_1'}{V_1}, \frac{\delta}{d_1}, \frac{V_1}{\sqrt{g\,d_1}}, \rho\frac{V_1 d_1}{\mu}, \frac{g\,\mu^4}{\rho\,\sigma^3}, ...\right) \quad (1)$$

where C is the void fraction, V is the velocity, u' is a characteristic turbulent velocity, d_{ab} is a characteristic size of entrained bubbles, F is the bubble count rate, x is the longitudinal coordinate measured from the upstream gate, y is the vertical elevation above the invert, z is the transverse coordinate measured from the channel centreline, x_1 is the distance between the jump toe and the upstream gate, d_1 is the inflow depth, V_1 is the inflow velocity, u_1' is a characteristic turbulent velocity at the inflow, δ is the boundary layer thickness of the inflow, g is the gravity acceleration, ρ and μ are the water density and dynamic viscosity respectively, and σ is the surface tension between air and water. In the right handside of Equation (1), the seventh, eighth and ninth terms are the inflow Froude Fr_1, Reynolds Re and Morton Mo numbers respectively. The Morton number is a function only of fluid properties and gravity constant. When the physical experiments are performed using the same fluids (air and water) in both model and prototype, the Morton number becomes an invariant.

In the present study, the turbulence and air entrainment in the hydraulic jump roller were investigated for relatively small upstream Froude numbers ($2.4 < Fr_1 < 5.1$). The laboratory experiments were conducted in a large size facility operating at large Reynolds numbers. These conditions are representative of some small full-scale treatment plant inlet and could be considered as a 10:1 scale study of a small to medium size storm waterway operation.

2. EXPERIMENTS AND INSTRUMENTATION

The experiments were performed in a horizontal rectangular flume. The channel width was 0.50 m. The sidewall height and the flume length were respectively 0.45 m and 3.2 m. The sidewalls were made of glass and the channel bed was PVC. The inflow conditions were controlled by a vertical gate with a semi-circular shape, and the gate opening was fixed at h = 0.036 m. The water discharge was measured with a Venturi meter located in the supply line and which was calibrated on-site. The clear-water flow depths were measured using rail mounted point gages with a 0.2 mm accuracy. The pressure and velocity measurements in steady supercritical flows were performed with a Prandtl-Pitot tube.

The air-water flow properties were measured with a double-tip conductivity probe. The dual-tip probe was equipped with two identical sensors with an inner diameter of 0.25 mm and separated by Δx_{tip} = 7.12 mm. The probe was excited by an electronic system (Ref. UQ82.518) designed with a response time of less than 10 μs. During the experiments, each probe sensor was sampled at 20 kHz for 45 s. The displacement and the position of the probe in the vertical direction were controlled by a fine adjustment system connected to a Mitutoyo™ digimatic scale unit (accuracy < 0.1 mm). Some photographic observations were performed using a Pentax™ K-7 camera. Further informations on the experiments were reported by Chachereau and Chanson (2010).

2.1. Experimental and inflow conditions

Two series of experiments were conducted. The first series focused on the general hydraulic jump properties. The experiments were performed with inflow Froude numbers between 2.4 and 5.1 corresponding to Reynolds numbers between 6.6×10^4 and 1.3×10^5. In the second series of experiments, some detailed air-water flow measurements at the sub-millimetric scale were conducted using the double-tip conductivity probe (Table 1). The flow conditions corresponded to Froude numbers between 3.1 and 5.1 and Reynolds numbers between 8.9×10^4 and 1.3×10^5. For all experiments, the jump toe was located at x_1 = 1.50 m from the upstream rounded gate. For these conditions, the inflow depth ranged from 0.044 down to 0.038 m depending upon the flow rate. The Prandtl-Pitot tube velocity data showed that the inflow was characterised by a partially-developed boundary layer. At the impingement point, the relative boundary thickness δ/d_1 ranged from 0.12 to 0.39 depending upon the flow rate.

Table 1 - Detailed air-water flow measurements in hydraulic jumps with relatively low Froude numbers

Ref.	B (m)	x_1 (m)	d_1 (m)	Fr_1	Re	$x-x_1$ (m)
Present study	0.5	1.50	0.0440	3.1	8.9×10^4	0.040 to 0.30
			0.0405	3.8	9.8×10^4	0.075 to 0.45
			0.0395	4.4	1.1×10^5	0.15 to 0.45
			0.0395	5.1	1.3×10^5	0.15 to 0.60
Chanson & Gualtieri (2009)	0.5	1.0	0.024	5.1	6.8×10^4	0.10 to 0.30
Murzyn & Chanson (2008)	0.5	0.75	0.018	5.1	3.8×10^4	0.075 to 0.225
Chanson & Gualtieri (2009)	0.25	0.50	0.012	5.1	2.5×10^4	0.02 to 0.10

3. BASIC OBSERVATIONS

Downstream of the jump toe, the free surface of the hydraulic jump was strongly turbulent (Fig. 1). At low inflow Froude numbers (Fr_1 < 2.3) the hydraulic jumps were undular: the front was followed by a train of secondary waves. For larger Froude numbers, the hydraulic jumps were characterised by a turbulent breaking roller. Some large vertical fluctuations, foamy air-water structures and water projections were observed. For the remaining sections, the inflow Froude number Fr_1 was larger than 2.4, corresponding to breaking jumps. They were characterised by a marked breaking roller, with some increasing air entrainment and air-water projections with increasing Froude number (Fig. 2). The upper spray region above hydraulic jumps was rarely investigated but for Chanson (2006) and Chanson and Chachereau (2010). The present observations highlighted a broad range of water and air-water droplet projections immediately above the jump toe, as well as some instantaneous discontinuity of the impingement perimeter. The high-shutter speed photographs and movies showed the large instantaneous air-water structures projected high above the roller surface. The short-lived structures exhibited a wide range of shapes (Fig. 2). While a large proportion of air-water structures were projected upwards with an initially forward motion, some were ejected with the negative direction, sometimes landing upstream of the jump toe. This was highlighted by droplet impacts on the camera lens (Fig. 2, Right).

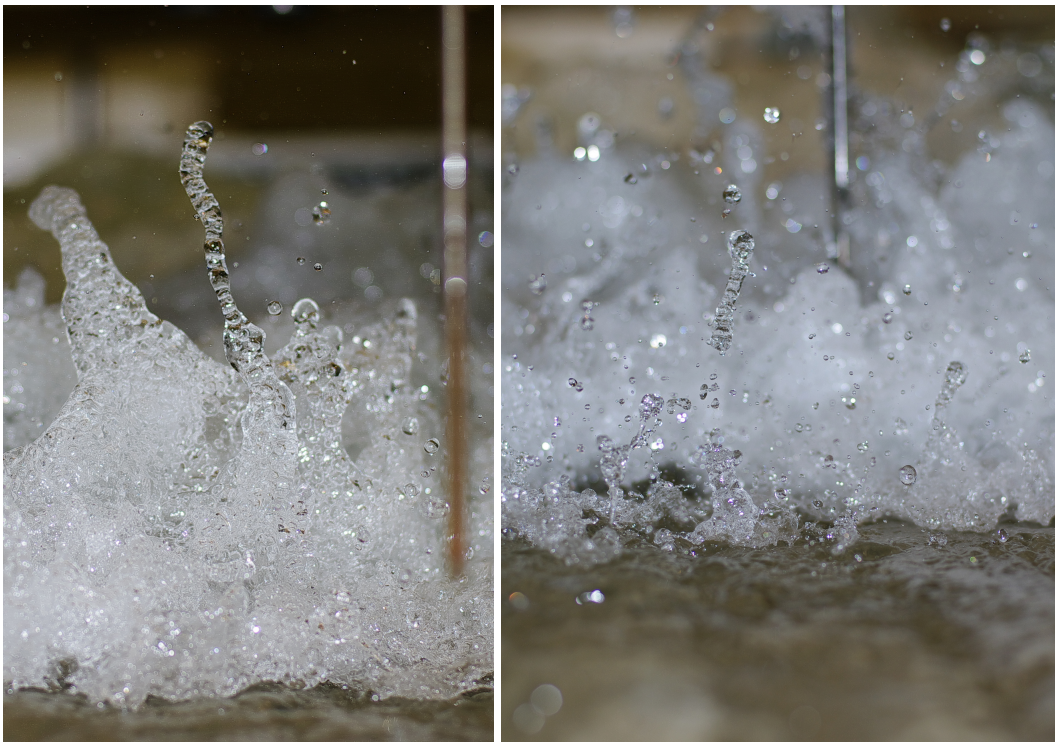

Fig. 2 - High-shutter speed photographs of air-water projections in hydraulic jumps, looking downstream at the impingement point and free-surface discontinuity at the jump toe - Flow from foreground to background - d_1 = 0.0395 / 0.0375 m, x_1 = 1.50 m, Fr_1 = 5.1 / 6.5, Re = 1.2 / 1.5×10^5 - Shutter: 1/180 s at f/2.5Fig. 4 - Dimensionless distributions of bubble count rate Fd_1/V_1 in a hydraulic jump for Fr_1 = 5.1, x_1/d_1 = 42, W/d_1 > 12 and Re = 25,000, 38,000, 68,000, 125,000 (Table 1) - Left: $(x-x_1)/d_1$ = 8; Right: $(x-x_1)/d_1$ = 12

4. AIR WATER FLOW PROPERTIES

In the hydraulic jump roller, two distinct air-water flow regions were identified: the lower region dominated by the developing turbulent shear layer; and the upper part consisting in the free surface region characterised by large void fraction, splashes and recirculation areas. Figure 3 presents some typical void fraction distributions in the roller of hydraulic jumps with partially-developed inflow conditions. The void fraction C reached a local maximum C_{max} in the air-water shear layer at an elevation y_{Cmax}, while the elevation y_* marked the vertical elevation above which the void fraction increased monotically to unity. In the developing shear layer, the void fraction data were compared successfully with an analytical solution of the advective diffusion equation for air bubble in a uniform flow (Chanson 1997,2010):

$$C = C_{max} \exp\left(- \frac{\left(\frac{y - y_{C\,max}}{d_1} \right)^2}{4D^{\#}\left(\frac{x - x_1}{d_1} \right)} \right) \quad (2)$$

where $D^{\#}$ is the dimensionless turbulent diffusivity assumed constant at a given longitudinal position, and d_1 and V_1 are respectively the inflow depth and velocity. Figure 3 presents some typical void fraction profiles at different longitudinal locations, and some data are compared with Equation (2). The dimensionless turbulent diffusivity $D^{\#}$ was deduced from the data best fit and ranged between 0.017 and 0.060. The results were basically independent of the longitudinal distance from the jump toe. although the finding differed from experimental data obtained in hydraulic jumps with large Froude

numbers (Chanson 2010). In the developing shear layer, the maximum void fraction C_{max} decreased with increasing distance from the impingement point ($x-x_1$) (Fig. 3). The data trend compared well with earlier experimental data (Murzyn et al. 2005, Chanson 2007,2010) for similar Froude numbers.

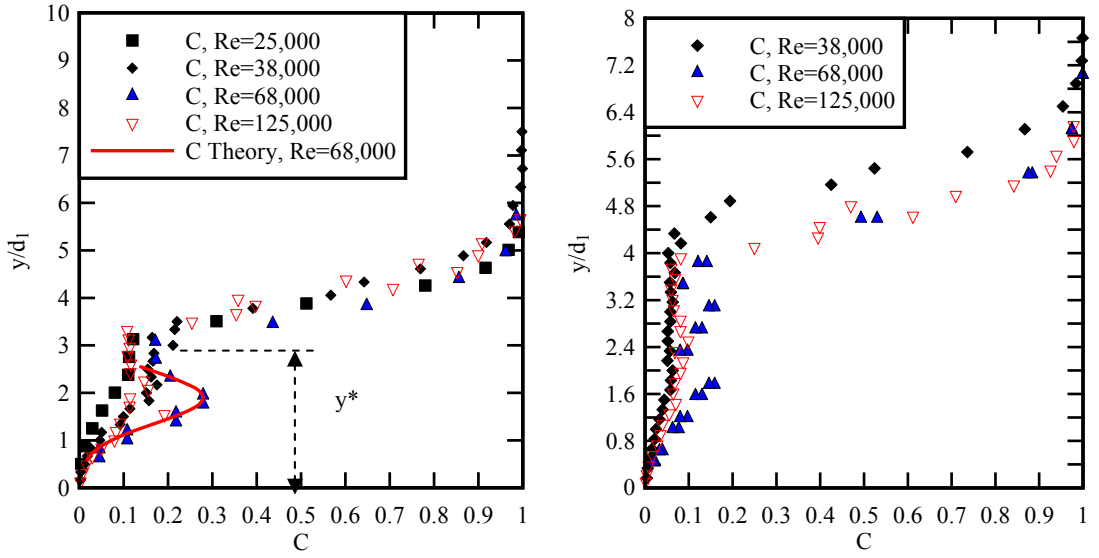

Fig. 3 - Dimensionless distributions of void fraction in a hydraulic jump for Fr_1 = 5.1, x_1/d_1 = 42, B/d_1 > 12 and Re = 25,000, 38,000, 68,000, 125,000 (Table 1) - Left: $(x-x_1)/d_1$ = 8; Right: $(x-x_1)/d_1$ = 12

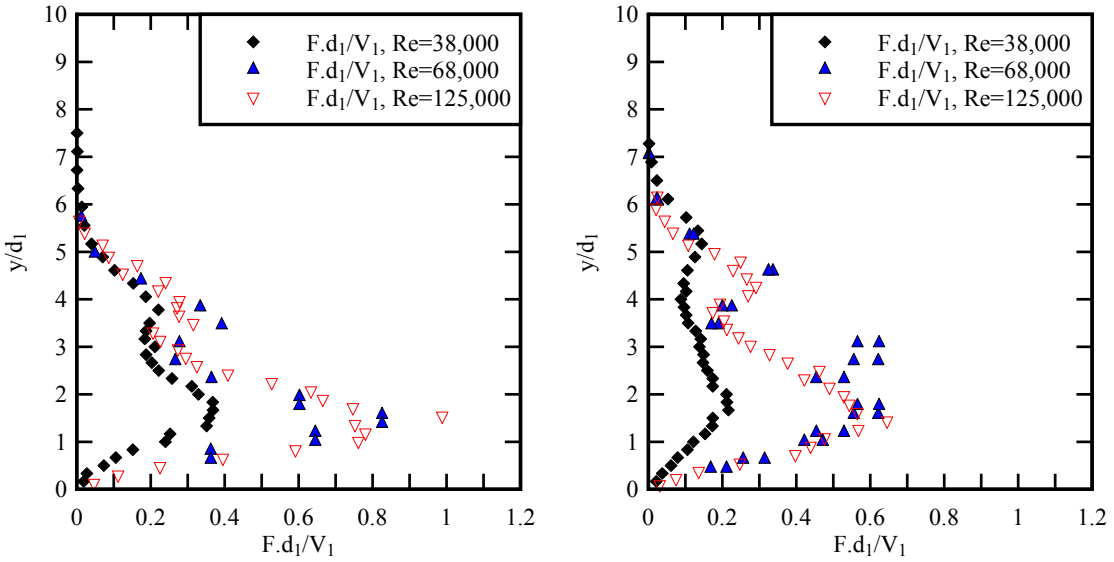

Fig. 4 - Dimensionless distributions of bubble count rate Fd_1/V_1 in a hydraulic jump for Fr_1 = 5.1, x_1/d_1 = 42, W/d_1 > 12 and Re = 25,000, 38,000, 68,000, 125,000 (Table 1) - Left: $(x-x_1)/d_1$ = 8; Right: $(x-x_1)/d_1$ = 12

The bubble count rate F, defined as the number of air bubbles detected by the probe sensor per unit time, was recorded for a range of experimental flow conditions. Figure 4 presents some typical vertical distributions of dimensionless bubble count rates. The data exhibited some profiles that were comparable to the earlier results of Chanson and Brattberg (2000), Murzyn et al. (2005), Chanson (2007), and Murzyn and Chanson (2008). They highlighted a maximum bubble count rate F_{max} in the air-water shear layer, linked with high levels of turbulent shear stresses that break up the entrained air bubbles into finer air entities. The experimental data showed that the maximum count rate decreased with increasing distance from the jump toe for a given inflow Froude number.

5. DYNAMIC SIMILARITY AND SCALE EFFECTS

The validity of the Froude similitude was tested for Fr_1 = 5.1 with respect to the two-phase flow properties. The present experiments were compared with the earlier data sets of Chanson and Gualtieri (2008) and Murzyn and Chanson (2008) (Table 1). The four data sets were geometrically similar based upon a Froude similitude with undistorted scale. The experiments were performed for Fr_1 = 5.1 with identical upstream distance x_1/d_1 between gate and jump toe, and the two-phase flow measurements were performed in the developing air-water flow region at identical dimensionless locations such that $(x-x_1)/d_1 < 15$. Typical comparative results are presented in Figures 3, 4 and 5. The data showed drastic scale effects in the smaller hydraulic jumps in terms of void fraction and bubble count rate distributions. The results highlighted consistently a more rapid de-aeration of the jump roller with decreasing Reynolds number for a given inflow Froude number for $Re < 6.8 \times 10^4$, an absence of self-similarity of the void fraction profiles in the developing shear layer for $Re < 4 \times 10^4$ (Fig. 3), and an increasing dimensionless bubble count rate with increasing Reynolds number for a given inflow Froude number (Fig. 4). In Figure 4, the bubble count rate data showed a monotonic increase in maximum bubble count rate $F_{max}d_1/V_1$ with no asymptotic trend within the range of investigated flow conditions.

In addition, some air-water turbulent properties showed also some scale effects, including in terms of turbulent intensities and integral time scales (Chachereau and Chanson 2010). In the air-water shear zone, the turbulence intensity was larger and the integral time scales were smaller for the largest Reynolds numbers, at the same given dimensionless location and for an identical Froude number. Further the bubble chord time distributions were not scaled according to a Froude similitude. Comparatively larger bubble chord times were observed at low Reynolds numbers. The present results supported the earlier findings (Chanson and Gualtieri 2008, Murzyn and Chanson 2008), and they extended the findings to a broader range of air-water flow properties and Reynolds numbers.

In hydraulic jumps, the level of clustering may give a measure of the magnitude of bubble-turbulence interactions and associated energy dissipation. For Fr_1 = 5.1, the effects of the Reynolds number were further tested on the bubble clustering properties. When two bubbles are closer than a particular length scale, they can be considered a group of bubbles: i.e., a cluster. Herein two bubbles were considered parts of a cluster when the water chord time between two consecutive bubbles was less than the bubble chord time of the lead particle. That is, the trailing bubble was in the near-wake of and could be influenced by the leading particle. Note that the criterion is based upon a comparison between the local, instantaneous characteristic time scales of the air-water flow. It did not rely upon the velocity measurement technique, but it implies that the streamwise velocity is positive. The criterion is also independent of the local air-water flow properties.

Some results are shown in Figure 5 in terms of the dimensionless number of clusters per second, and the number of bubbles per cluster. Basically the dimensionless properties of bubble clusters in the air-water shear layers were not scaled according to a Froude similitude. The comparative analysis showed that the dimensionless number of clusters per second, the percentage of bubbles in cluster and the number of bubbles per clusters increased monotically with the Reynolds number at a given dimensionless location $(x-x_1)/d_1$ and for a given Froude number. The present findings highlighted that the clustering affected a comparatively greater proportion of bubbles at high Reynolds numbers, indicating that the interactions between entrained bubbles and vortical structures were not scaled accurately with the Froude similarity.

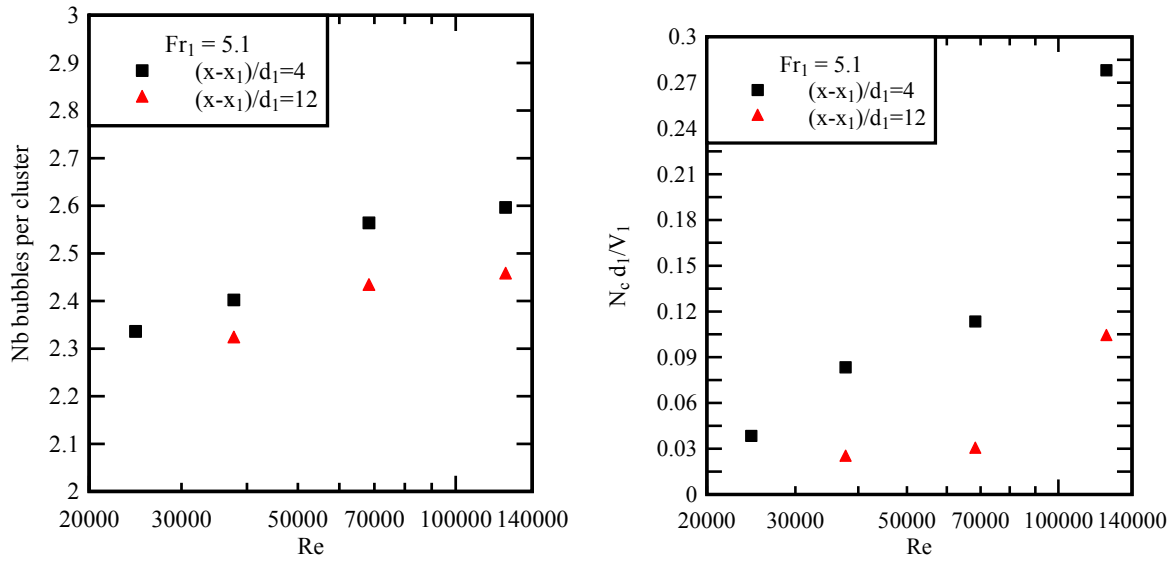

Fig. 5 - Effects of the Reynolds number on the bubble cluster properties in the air-water shear layer of hydraulic jumps at the locations where $F = F_{max}$ ($y = y_{Fmax}$) - $Fr_1 = 5.1$, $(x-x_1)/d_1 = 4$ & 12 (Table 1)

6. CONCLUSION

The hydraulic jump is a complex phenomenon that remains incompletely understood. In the present study, both the air-water flow patterns and the air-water properties were investigated experimentally in hydraulic jumps with relatively small Froude numbers ($2.4 < Fr_1 < 5.1$) and relatively large Reynolds numbers ($6.6\times10^4 < Re < 1.3\times10^5$). The air-water flow measurements indicated that the vertical profiles of void fraction showed two characteristic regions: the air-water shear layer in the lower part of the jump and an upper free-surface region above. The air-water shear zone was characterised by local maxima in terms of void fraction and bubble count rate. The comparative analysis demonstrated that, for hydraulic jumps with $Fr_1 = 5.1$, the void fraction data obtained with $Re < 4\times10^4$ could not be scaled up to $Re = 1\times10^5$. Further the bubble count rate data, turbulence properties, bubble chords and clustering properties with Reynolds numbers up to 1.25×10^5 could not be up-scaled to large-size prototype structures without significant scale effects in terms of bubble count rate, turbulence and bubble chord time distributions.

The findings have some major implications of civil, environmental and sanitary engineering, because most hydraulic structures, storm water systems and water treatment facilities operate with Reynolds numbers within ranging from 10^6 to over 10^8. In a physical model, the flow conditions are said to be similar to those in the prototype flow conditions if the model displays similarity of form, similarity of motion and similarity of forces. The present results demonstrated quantitatively that the dynamic similarity of two-phase flows in hydraulic jumps at relatively small Froude numbers cannot be achieved with a Froude similarity unless working at full-scale.

7. REFERENCES

Chachereau, Y., and Chanson, H., (2010). *Free-Surface Turbulent Fluctuations and Air-Water Flow Measurements in Hydraulics Jumps with Small Inflow Froude Numbers*. Hydraulic Model Report No. CH78/10, School of Civil Engineering, The University of Queensland, Brisbane, Australia, 133 pages.

Chanson, H. (1997). *Air Bubble Entrainment in Free-Surface Turbulent Shear Flows*. Academic Press, London, UK, 401 pages.

Chanson, H. (2006). *Bubble Entrainment, Spray and Splashing at Hydraulic Jumps*. Journal of Zhejiang University SCIENCE A, Vol. 7, No. 8, pp. 1396-1405.

Chanson, H. (2007). *Bubbly Flow Structure in Hydraulic Jump*. European Journal of Mechanics B/Fluids, Vol. 26, No. 3, pp.367-384 (DOI: 10.1016/j.euromechflu.2006.08.001).

Chanson, H. (2009a). *Current Knowledge In Hydraulic Jumps And Related Phenomena. A Survey of Experimental Results*. European Journal of Mechanics B/Fluids, Vol. 28, No. 2, pp. 191-210 (DOI: 10.1016/j.euromechflu.2008.06.004).

Chanson, H. (2010). *Convective Transport of Air Bubbles in Strong Hydraulic Jumps*. International Journal of Multiphase Flow, Vol. 36, No. 10, pp. 798-814 (DOI: 10.1016/j.ijmultiphaseflow.2010.05.006).

Chanson, H., and Brattberg, T. (2000). *Experimental Study of the Air-Water Shear Flow in a Hydraulic Jump*. International Journal of Multiphase Flow, Vol. 26, No. 4, pp. 583-607.

Chanson, H., and Chachereau (2010). *Air Bubble Entrainment and Water Projections in Hydraulic Jumps*. 7th International Conference on Multiphase Flow ICMF 2010, Tampa FL, USA, May 30-June 4, Gallery of Multiphase Flow, Poster presentation.

Chanson, H., and Gualtieri, C. (2008). *Similitude and Scale Effects of Air Entrainment in Hydraulic Jumps*. Journal of Hydraulic Research, IAHR, Vol. 46, No. 1, pp. 35-44.

Hager, W.H. (1992). *Energy Dissipators and Hydraulic Jump*. Kluwer Academic Publ., Water Science and Technology Library, Vol. 8, Dordrecht, The Netherlands, 288 pages.

Henderson, F.M. (1966). *Open Channel Flow*. MacMillan Company, New York, USA.

Mossa, M., and Tolve, U. (1998). *Flow Visualization in Bubbly Two-Phase Hydraulic Jump*. Jl Fluids Eng., ASME, Vol. 120, March, pp. 160-165.

Murzyn, F., and Chanson, H. (2008). *Experimental Assessment of Scale Effects Affecting Two-Phase Flow Properties in Hydraulic Jumps*. Experiments in Fluids, Vol. 45, No. 3, pp. 513-521 (DOI: 10.1007/s00348-008-0494-4).

Murzyn, F., Mouaze, D., and Chaplin, J.R. (2005). *Optical Fibre Probe Measurements of Bubbly Flow in Hydraulic Jumps*. International Journal of Multiphase Flow, Vol. 31, No. 1, pp. 141-154.

Rajaratnam, N. (1962). *An Experimental Study of Air Entrainment Characteristics of the Hydraulic Jump*. Journal of Instn. Eng. India, Vol. 42, No. 7, March, pp. 247-273.